Effect of the Pt-Pd molar ratio bimetallic catalysts supported on sulfated zirconia in the gas-phase hydrodechlorination of chloromethanes

J. Bedia[a*], A. Arevalo-Bastante[a], J.M. Grau[b], L.A. Dosso[b,] J.J. Rodríguez[a], A. Mayoral[c], I. Diaz[d], L.M. Gómez-Sainero[a]

[a] Sección de Ingeniería Química, Universidad Autónoma de Madrid, Cantoblanco, 28049 Madrid, Spain.
[b] Instituto de Investigaciones en Catálisis y Petroquímica "Ing José Miguel Parera" - INCAPE - (FIQ-UNL, CONICET), CCT CONICET Santa Fe "Dr. Alberto Cassano". Colec. Ruta Nac. Nº 168 KM 0 Paraje El Pozo, S3000AOJ, Santa Fe, Argentina.
[c]Laboratorio de Microscopía Avanzada, Instituto de Nanociencia de Aragón, Universidad de Zaragoza, 50018, Zaragoza, Spain.
[d]Instituto de Catálisis y Petroleoquímica, CSIC, 28049, Madrid, Spain.

*Telephone number: 34 91 4972911. Fax number: 34 91 4973516.
E-mail: jorge.bedia@uam.es.

Abstract.

Bimetallic Pt:Pd catalysts with different molar ratios and 0.5 wt% overall metal load supported on sulfated zirconia catalysts (SZ) were synthesized and tested in the gas-phase hydrodechlorination (HDC) of chloromethanes and their mixtures. The catalysts were characterized by adsorption-desorption of N_2 at -196 ºC, X-ray diffraction, X-ray photoelectronic spectroscopy, temperature programmed reduction and aberration corrected scanning transmission electron microscopy (STEM). The effect of the Pt:Pd molar ratio on the activity, stability and selectivity was analyzed. The high acidity of the sulfated zirconia results in metal particles of small size (mainly < 5 nm) as confirmed by STEM. The bimetallic catalysts showed higher stability than the monometallic ones as demonstrated in long term experiments (80 h on stream), confirming the positive effect

of combining both metallic phases. TOF values in the range of 0.0007 to 0.0168 s^{-1} and apparent activation energies between $\approx$ 41-44 kJ·mol^{-1} were obtained. TOF values for dichloromethane HDC increased at increasing mean metal particle size within the range of this work ($\approx$1.2-2.3 nm). The catalysts with Pt:Pd molar ratios of 1:3 and 1:1 showed significantly better performance than the 3:1 one for overall dechlorination due to their higher atomic metal content and TOF at the same total metal weight load (0.5%).

1. Introduction

Chlorinated volatile organic compounds (CVOCs) emissions promote photochemical smog formation, ozone depletion, and global warming [1]. Catalytic hydrodechlorination (HDC) of CVOCs has been extensively studied in the last years, using catalysts with different metals and supports. The stability of these catalysts is crucial regarding potential application. However, many studies focused on gas-phase hydrodechlorination of chlorometanes, such as dichloromethane (DCM) and chloroform (TCM), using supported metallic catalysts do not include stability tests or they report a rapid deactivation of the catalysts [2,3,4,5,6]. The literature presents different explanations for that deactivation, namely, poisoning by chlorinated organic species and/or HCl, coke formation, metal sintering or changes in the metal oxidation state [7,8,9,10,11]. In the last years, in order to increase the activity and/or stability, or modulate the selectivity, the use of bimetallic catalysts has been more in-depth investigated. Compared to monometallic catalysts, the bimetallic ones are usually more stable upon time-on-stream, because they are more resistant to HCl poisoning [12,13]. Furthermore, the addition of a second noble metal or a transition metal to a noble metal catalyst improves its activity [13,14] or the selectivity to certain reaction products [15,16]. One of the reasons reported for the better behavior of the bimetallic catalyst is the improved dispersion of the active phase as a consequence of the interaction between the two metals [17,18,19].

In a previous work [20], we tested monometallic (Pt or Pd) and bimetallic (Pt-Pd) catalysts supported on zirconia promoted with sulfate (SZ) in the gas-phase hydrodechlorination of dichloromethane. The catalysts prepared showed high activity and selectivity to non-chlorinated products (between 80 and 90 % at 250 ºC) being methane the main reaction product. It was observed that the presence of palladium improved the stability of the catalysts in long-term experiments (80 h on stream). The catalyst with the

highest metal dispersion showed also the highest stability (no deactivation after more than 80 h on stream) which suggests that metal particle size is relevant in that respect. However, the effect of the relative proportion of both metals in the performance of the catalyst was not evaluated, and mixtures of chloromethanes were not tested, despite the residual gas streams containing those species commonly include several of them.

In the current study, we analyze the effect of the molar ratio of Pd-Pt on sulfated zirconia catalysts in the gas-phase hydrodechlorination of chloromethanes and their mixtures. The results, in terms of activity and stability, are compared with those obtained previously using monometallic catalysts [20]. Moreover, the presence of bimetallic metal particles was confirmed by a wide investigation through spherical aberration corrected (C_s-corrected) Scanning Transmission Electron Microscopy (STEM).

2. Experimental

2.1. Catalyst preparation

The preparation procedure is reported elsewhere [20]. Briefly, monometallic (Pt or Pd) and bimetallic (Pt and Pd) catalysts with different Pt:Pd molar ratios were supported on a sulfate-promoted zirconia. The support used to prepare the catalysts was a commercial sample supplied by MEL Chemicals. SO_4^{2-}–ZrO_2 (XZO 1248, 7 % SO_3, > 300 m^2 g^{-1}, > 0.3 ml g^{-1}, 1 μm particle size) in the form of powdered hydroxide gel (SZOH). It was first conditioned by calcination at 600 °C (SZ) in air. The calcined support was then impregnated by the incipient wetness method with aqueous solutions of the metallic precursors, chloroplatinic acid ($H_2Cl_6Pt \cdot 6H_2O$, Sigma-Aldrich, <99.9%, CAS Number: 26023-84-7) and/or palladium chloride (Cl_2Pd, Sigma-Aldrich, <99.9%, CAS Number: 7647-10-1). The solution concentration was adjusted to obtain a total nominal content of active phase (Pt + Pd) of 0.5 wt%, with different Pt:Pd molar ratios in the case of the

bimetallic catalysts (1:3, 1:1 and 3:1). Once the samples were impregnated, they were maintained 24 h at room temperature and then dried slowly in a stove. The temperature was slowly raised from ambient to 110 ℃ in order to prevent solvent carrying over the metal precursor to the pore mouths. The samples obtained were denoted as SZ-Pd and SZ-Pt for the palladium and platinum monometallic sulfated zirconia, respectively. In the case of the bimetallic catalysts, the SZ was impregnated first with a chloroplatinic acid solution by the incipient wetness method and afterwards with palladium chloride. The samples obtained were named SZ Pd-Pt (1:3), SZ Pd-Pt (1:1) and SZ Pd-Pt (3:1) according to the Pt:Pd molar ratio.

2.2. Catalyst characterization

N_2 adsorption–desorption at -196 ℃ (Micromeritics TriStar apparatus) was used to characterize the porous texture of the catalysts. The samples were previously outgassed for at least 8 h at 150 ℃ at a residual pressure of 10^{-3} Torr. The BET equation [21] was used to calculate the total surface area of the samples, and the pore volume was obtained from the amount of nitrogen adsorbed at a relative pressure of 0.95 (calculated as liquid). The reducibility of the palladium and platinum metallic phases of the catalysts was assessed from temperature programed reduction (TPR) analyses. These tests were carried out in an Ohkura TP2002 equipment using a thermal conductivity detector. A sample of 150 mg of catalyst was first calcined at 450 ℃ under air flow, followed by a stabilization in Ar at 100 ℃ and cooling down to room temperature. Finally, the samples were heated up to 800 ℃ at 10 ℃·min^{-1} under continuous flow of hydrogen (4.8%) in Ar.

The crystalline structure of the catalysts was analyzed by X-ray diffraction (XRD) in a X'Pert PRO Panalytical Diffractometer using Cu Kα monochromatic radiation (λ =

0.15406 nm) and a Ge mono filter. A scanning range of 2θ = 20-75° was covered with scan step size of 0.020° and 5 s collection time.

The mass surface composition and the oxidation state of the metallic phase of the catalysts was studied by X-ray photoelectron spectroscopy (XPS) using a Physical Electronics 5700C Multitechnique System, using Mg Kα radiation (hυ = 1253.6 eV) apparatus. Binding energy values were adjusted taking into account the effects of sample charging by placing the C1s peak (284.6 eV) as an internal standard. The deconvolution procedure involved smoothing, a Shirley background subtraction and curve fitting using mixed Gaussian–Lorentzian functions by a least squares method.

Transmission electron microscopy (TEM) analyses were carried out using an aberration corrected FEI-TITAN transmission electron microscope operated at 300 kV allowing a point resolution of 0.8 Å. The microscope, corrected for the electron probe, was operated in scanning mode (STEM) using a high angle annular dark field detector (HAADF) and it was equipped with an EDS detector (EDAX) for chemical analysis. The samples were dispersed in ethanol and dropped onto holey carbon-coated Cu grids.

All the characterization was performed on the catalysts calcined and then reduced under the same conditions used in the catalytic activity experiments (except for TPR, where the catalysts were only calcined).

2.3. Catalytic HDC experiments

The activity and stability of the catalysts in the gas-phase hydrodechlorination of chloromethanes were evaluated in a continuous flow reaction system described elsewhere [20], consisting basically of a 4.0 mm i.d. quartz fixed bed micro-reactor (Microactivity Reference, PID Eng&Tech, Spain) coupled to a gas chromatograph (Varian, model 450GC) equipped with a FID detector and a capillary column (Varian, CP-SilicaPLOT,

60 m) for the analysis of the exit stream. The catalysts were treated "in situ" by calcination in air at 450 ºC (50 Ncm^3 min^{-1}) and reduction in hydrogen stream (50 Ncm^3 min^{-1}) for 1 h at 300 ºC prior to the reaction. The experiments were performed at atmospheric pressure using an inlet total flow rate of 100 Ncm^3 min^{-1} and a H$_2$/CM (chloromethane) molar ratio of 100 at 0.8 kg$_{cat}$·h·(mol CM)$^{-1}$ space time. The gas feed contained a CM concentration of 1000 ppmv and was prepared by mixing appropriate proportions of a commercial mixture of chloromethanes and N$_2$ (4000 ppmv of CM in N$_2$) with pure N$_2$. Reaction temperatures within the range of 150–250º C were tested. For the sake of checking possible mass-transfer limitations, previous experiments were performed at 250 ºC varying the total flow rate and the catalyst particle size. No significant changes were found in CM conversions for gas velocities and catalyst particle sizes within the ranges of 0.02–0.06 m/s and 0.25–0.71 mm, respectively. The behavior of the catalysts was analyzed in terms of CM conversion (X), selectivity to the different reaction products (S$_i$), turnover frecuency (TOF) and overall dechlorination. The values of turnover frequency were calculated as the moles of reactant converted per mol of surface exposed metal atoms (Pt plus Pd). The dispersion values were calculated using the equations dp$_{Pd}$ (nm) = 112.1/D(%) and dp$_{Pt}$ (nm) = 113.2/D(%) [22], assuming spherical metallic particles and being dp the corresponding mean particles sizes obtained by TEM. The amount of exposed metal atoms was calculated from the nominal content of palladium and platinum in µmol per gram of catalysts multiplied by the corresponding dispersion values. The evolution of the catalytic activity upon time on stream was also studied. The carbon mass balances were checked and they matched always within 91–99% once the stationary state was reached. The experimental results were reproducible with less than 5% error.

3. Results and discussion

3.1. Catalysts characterization

Figure 1 shows the TPR profiles of the catalysts. These profiles contain only the peaks associated with the reduction of the metallic species, namely, platinum and palladium. SZ Pt displays a single peak associated to the reduction of the platinum species at 166 °C. On the other hand, the TPR profile of SZ Pd shows a peak centered at 102 °C with a shoulder at 116 °C, related to the reduction of palladium. Modifications of the interaction between the oxidized species and the support give rise to changes in the reduction temperatures. Since these changes were towards higher values, this suggests a higher stability of the oxide phase, either intrinsically more stable or stabilized by the support. TPR profiles of the bimetallic catalysts also show a single peak in spite of the presence of the two metals. That suggests some type of interaction between both, as previously observed with other supports [23,24]. Probably palladium, which is reduced at lower temperature, can provide dissociated hydrogen for the reduction of platinum, and therefore is reduced at lower temperature than in the monometallic SZ Pt catalyst.

(Figure 1)

Figure ES1 (Electronic Supplementary Information) represents the N_2 adsorption-desorption isotherms of the catalysts at -196 °C. They can be associated to type IV of IUPAC classification, characteristic of mesoporous materials. The low amount of nitrogen adsorbed at low relative pressures indicates a low contribution of microporosity. The differences between the isotherms of the different catalysts are negligible. All the catalysts yielded BET surface areas in the vicinity of 115 m^2/g with total pore volumes of around 0.175 cm^3/g.

Table 1 summarizes the nominal bulk platinum and palladium mass contents and the Pt^0/Pt^{n+} atomic ratio on the surface of the catalysts obtained from deconvolution of the Pt 4f XPS region (see Figure ES2). It was not possible to analyze unambiguously the Pd 3d signal due to the overlapping of the Pd $3d_{5/2}$ and Zr $3p_{3/2}$ signals [25] and the much higher surface concentration of zirconia (76-78 wt% versus 0.3-1.1 wt% of palladium). Therefore, no information about external Pd could be obtained. The Pt^0/Pt^{n+} values suggest that platinum on the outermost surface is mainly in the zerovalent state, most probably due to the reduction with H_2 prior to HDC reaction.

(Table 1)

The XRD profiles of the fresh catalysts are depicted in Figure ES3, showing the main peaks associated to tetragonal ($t-ZrO_2$) and monoclinic ($m-ZrO_2$) phases of zirconia [26]. Peaks related to other crystalline species are not observed, suggesting that the Pt and Pd particles are too small to produce any reflection. Figure ES4 depicts a magnification of the XRD spectra in the 2θ range of 39-41º, where the peaks of metallic (zero-valent) platinum and palladium (39.8º and 40.1º, respectively [27]) are not observed suggesting that the metal particles are relatively well dispersed. The high acidity of the sulfated zirconia support could explain the low metal particle size (as it will be corroborated later on by the electron microscopy observations) since the presence of acidic groups increases the hydrophilic character of the support and favors the diffusion of the metal precursor [28,29,30]. The XRD pattern of the SZ Pt-Pd (1:3) catalyst after reaction in the long-term experiment of TCM hydrodechlorination showed no significant changes when compared with those of the fresh or reduced catalysts (Figure ES5). This indicates that the used

catalyst did not suffer significant modifications of the metal particle size during the reaction.

The bimetallic catalysts were further analyzed by advanced electron microscopy methods. For this study, C_s-corrected STEM-HAADF was used with the intention of obtaining atomic-resolution information [31] and due to its high sensitivity to the atomic number of the elements allowing a clear visualization of metals in lighter supports [32]. Figure 2 shows representative C_s-corrected STEM images of the SZ Pt-Pd (1:1) and SZ Pt-Pd (1:3) catalysts and the corresponding EDS analyses that confirm the presence of both metals. The STEM-HAADF images (Figures 2a and c) display very well dispersed metallic particles (observed as bright spots due to their higher scattering factor) over the zirconia substrate. Interestingly, in the case of SZ Pt-Pd (3:1), although it is mainly observed the presence of well dispersed metal nanoparticles (as for the other bimetallic catalysts) also exist some significantly larger metallic clusters of nanoparticles with sizes up to tenths of nm as shown in the STEM-HAADF image depicted in Figure 3. Nevertheless, these bigger metallic aggregates, are very low in number.

(Figure 2)

(Figure 3)

A closer inspection of SZ Pt-Pd (1:1) is presented in Figure 4. Figure 4a shows several nanoparticles with *fcc* symmetry together with disordered metallic clusters. In a more magnified image (Figure 4b) a 2 nm *fcc* nanoparticle can be identified in addition to isolated metal atoms (denoted by red arrows). The structure of the support proving its good crystallinity can be observed in Figures 4c and 4d. A lower magnification micrograph of an entire ZrO_2 particle is shown in Figure 4c where the metal nanoparticles

are marked by red arrows. The atomic-resolution image of 4c is presented in 4d confirming the $P121\,c1$ space group; the FFT that can be indexed assuming this space group is shown inset. A closer observation of the Zr-Zr dumbbells, separated by only 0.7 Å, are shown inset together with the structural model (where Zr appears in green and O in red).

(Figure 4)

The size distribution of Pt-Pd nanoparticles of the different bimetallic catalysts is given in Figure ES6, without considering the very few clusters of nanoparticles (tenths of nm) observed in SZ Pt-Pd (3:1). The lowest mean particle size is 1.3±0.3 nm for SZ Pt-Pd (3:1), followed by 1.9±0.6 nm for SZ Pt:Pd (1:3) and finally, SZ Pt:Pd (1:1) catalyst with 2.3±0.9 nm. This low particle size pattern observed for all the samples is consistent with the aforementioned absence of peaks in the XRD profiles of the different catalysts.

Figure 5 shows different magnification C_s-corrected STEM images of SZ Pt-Pd (1:1) after used in long term HDC experiment. As can be seen, the metallic particles (bright spots) maintain the initial homogeneous size distribution on the support. Furthermore, the particle size distribution of the used catalyst (Figure ES7) is relatively similar to that of the fresh one (Figure ES6), the mean size increasing only from 2.27 nm to 2.81 nm after used in reaction.

(Figure 5)

3.2. Catalytic activity

Figure 6 depicts the evolution of dichloromethane (DCM) conversion upon time on stream (tos) in long-term experiments at 0.8 $kg_{cat} \cdot h \cdot mol^{-1}$ space time and at 250 ºC. All the

catalysts yielded similar initial conversion values, except SZ Pt-Pd (3:1). All the bimetallic catalysts showed a fairly good stability, somewhat better than that of the monometallic Pd catalyst (SZ Pd), while the platinum one (SZ Pt) suffered a rapid and strong deactivation. Deactivation of catalysts in HDC has been attributed to different causes, namely, poisoning by HCl, deposition of coke or organochlorinated species, metal sintering, changes in the oxidation states of metal or loss of metal because of volatilization. Since no significant changes were observed in the XRD profiles of the different catalysts before and after reaction, it is not likely metal sintering cause catalyst deactivation. In a previous study [20] we reported an increase in the carbon content of the catalysts after reaction, suggesting that partial blockage of active sites could be a possible cause of deactivation. However, in the case of the SZ Pt catalyst, it was observed a very significant reduction of the sulfur content, which can be due to the reduction of $SO_4^=$ to SO_2, further reduced to H_2S in the presence of Pt. This H_2S could poison Pt sites, thus explaining the lower stability of the SZ Pt catalyst. In contrast, the presence of bimetallic particles favors the stability of the catalysts. It is noteworthy the decrease of conversion at low times on stream with all the bimetallic catalysts in more or less extent. This suggests some type of surface restructuration, as could indicate the small changes observed in the TEM analyses of those catalysts before and after reaction. According to previous works [23,33], the presence of HCl could result in the volatilization of metallic chlorides, reduction under H_2 atmosphere and later metal deposition giving rise to that surface restructuration. SZ Pt-Pd (1:3) and SZ Pt-Pd (1:1) yielded significantly higher DCM conversion than SZ Pt-Pd (3:1) (Figure 6). Despite metal dispersion is slightly higher for the latter, (as will be shown below, Table 2), this can be attributed to the lower atomic metal loading of SZ Pt-Pd (3:1), as a consequence of its higher Pt proportion (all the catalysts have an overall weight metal content of 0.5%) and TOF values.

(Figure 6)

Figure 7 shows the results obtained at different temperatures with the highly stable SZ Pt-Pd (1:3) catalyst in the hydrodechlorination of DCM at 1000 ppmv inlet concentration and 0.8 $kg_{cat} \cdot h \cdot mol^{-1}$ space time. The results corresponding to the rest of the bimetallic catalysts are reported as Supplementary Information (Figures ES8 and ES9). The selectivities observed followed similar patterns with all the catalysts tested. The following non-chlorinated products were detected: methane, ethane, propane, n-butane and 1-butene, being methane by far the most abundant. The only chlorinated product was monochloromethane (MCM) and the selectivity to it decreased at increasing reaction temperature and, consequently, at increasing DCM conversion. In all cases, a substantial increase of DCM conversion was observed at increasing temperatures but obtaining high overall dechlorination requires the operation at the highest temperature tested (250 ºC).

(Figure 7)

The selectivities to the different reaction products did not suffer significant modifications upon time on stream, remaining almost constant after an initial transition period as can be seen in Figure 8 for SZ Pt-Pd (1:3) at 250 ºC. In a previous study using a Pd on activated carbon catalyst, Martin-Martinez et al. [34] reported fairly similar DCM conversion and selectivity to MCM although with lower stability. Using Pt on activated carbon these authors obtained significantly lower values of DCM conversion and higher selectivities to MCM (thus lower dechlorination degree) but the catalyst showed a high stability as well as the bimetallic catalyst of the current work.

(Figure 8)

Figure 9 shows the results obtained with the SZ Pt-Pd (1:3) catalyst at different reaction temperatures in the HDC of chloroform (TCM). As can be seen, TCM conversions are significantly higher than those obtained for DCM under the same conditions (Figure 6) due to its higher reactivity [35,36]. Fairly high conversion was achieved even at the lowest temperature tested (150 ℃), reaching 97% at 250 ℃. The selectivities to chlorinated byproducts (DCM and MCM) was very low (about 1.8% at 250 ℃) thus meaning a high overall dechlorination. Again, the main reaction product was by far methane, although ethane and propane were also obtained in significant amounts, especially the former (more than 12% selectivity at 250 ℃).

(Figure 9)

Figure 10 shows the evolution of TCM conversion and selectivities to the different reaction products upon time on stream with the SZ Pt-Pd (1:3) catalyst at a space time of 0.8 $kg_{cat} \cdot h \cdot mol^{-1}$ and 250 ℃. Again, the catalyst is also quite stable, although in this case a slow but continuous loss of activity can be observed. Selectivities did not suffer significant changes during time on stream. The main product was by far methane, with around 80% selectivity, followed by ethane ($\approx$ 16%). The selectivity to chlorinated products, namely DCM and MCM, remained very low (bellow 1%) along the experiment.

(Figure 10)

14

Figures 7 and 9 include the TOF values obtained in the HDC of DCM and TCM, respectively, with the SZ Pt-Pd (1:3) catalyst at different temperatures. Those values were significantly higher for TCM, because of its higher reactivity [35,36]. Analogous Figures are given as supporting information (ES9 and 10) for the two other bimetallic catalysts tested in the HDC of DCM. Table 2 summarizes the number of exposed sites of Pd and Pt for the bimetallic catalysts and the TOF values for the HDC of DCM with the three catalysts at all the temperatures tested. TOF values in the range of 0.0007 to 0.0168 s^{-1} were obtained. González-Sánchez et al. [6] reported TOF values for the HDC of DCM with Pd catalysts supported on alumina and sol-gel titania. The former showed a higher activity, with a TOF value of 0.0025 s^{-1} at 200 ºC, lower than the 0.0029-0.0075 s^{-1} obtained with our catalysts. Our research group has previously reported [19] TOF values for this reaction with carbon-supported Pd–Pt catalysts. Those values were in the range of 0.0278-0.0335 s^{-1} at 175 ºC, higher than the reported in the current work. Bonarowska et al [37] analyzed also the HDC of DCM on Pd–Re/Al_2O_3 catalysts obtaining TOF values between 0.0170 and 0.0754 s^{-1}.

Figure 11 shows the TOF values for the HDC of DCM at 200 ºC versus the mean metal - particle size (TEM) of the three bimetallic catalysts. An increase of TOF at increasing particle size can be observed, within the range of the Figure. Moreover, the lower TOF value corresponds to the catalyst with the highest proportion of Pt, in agreement with previous results [19]. The different proportion of both metals or the slight differences founded in the oxidation states (see Pt^0/Pt^{n+} values of Table 1) showed no significant effect on the TOF values, also in agreement with previous results for carbon supported bimetallic Pd-Pt catalyst [19].

Table 2 includes the values of apparent activation energy for the HDC of DCM with the three bimetallic catalysts. Fairly close values ($\approx$ 41-44 kJ·mol^{-1}) were obtained. These

values are lower (in some cases significantly lower) than other previously reported in the literature for the same reaction with different catalysts. Bonarowska et al. [37] obtained activation energies in the range of 51.1-65.5 kJ·mol^{-1} with Pd–Re/Al$_2$O$_3$ catalysts. Gonzalez-Sanchez et al. [6] reported much higher values of activation energy (92.5-130.9 kJ·mol^{-1}) for the HDC of DCM in the presence of traces of other chlorometanes on Pd supported with commercial alumina or sol–gel titania. In contrast, the values obtained in the current work are close to the reported by Alvarez-Montero el al. [38] with a Pt on activated carbon (45.1 kJ·mol^{-1}) or by López et al. [39], who obtained 41.1 kJ·mol^{-1} with a Pd/Al$_2$O$_3$ catalyst.

(Table 2)

(Figure 11)

Finally, the performance of SZ Pt:Pd (1:3) in the HDC of mixtures of chloromethanes was also analyzed. Few studies deal with the HDC of mixtures of chloromethanes [5,6,40,41] although, in many cases, these compounds are released together in residual gas streams [39]. Figure 12 shows the results obtained in the HDC of mixtures of (a) TCM and DCM and (b) tetrachloromethane (TTCM), TCM, DCM and monochloromethane (MCM) at 250 ºC. As can be seen, in both cases, the catalyst showed a fairly stable behavior after an initial transition period. The steady state transformation of the different chloromethanes was directly related to the number of chlorine atoms in the molecule (TTCM>TCM>DCM>MCM). With the TCM and DCM mixture (Figure 12a), the catalyst yielded complete conversion of TCM with close to 75% overall dechlorination. Using the mixture of the four chloromethanes (Figure 12b), complete conversion of TTCM and TCM was achieved, while significant concentrations of DCM and MCM in

the exit stream were remaining. An overall dechloration of almost 80% was maintained along the 35 h of the experiment. The main reaction product was methane, with much lower amounts of other alkanes, namely, ethane and propane. This results confirm the high stability of the catalyst synthesized in the HDC reaction, even when dealing with complex mixtures of chloromethanes. It is observed a reduction of the DCM conversion values when the reaction takes place in the presence of TCM, which suggests the existence of some type of inhibition effect. This behavior is in agreement with previous observations on the competition between the different reactants for the active centers of the catalysts [6,40]. When four different CMs were used, a significant decrease of the DCM conversion was found, with respect to that obtained under the same conditions using this compound alone or accompanied by TCM. This supports the existence of some inhibitory effect. To identify in detail those effects would require further research given the fairly different reactivities of the four CMs used (TTCM>TCM>DCM>MCM [36]).

(Figure 12)

Conclusions

Bimetallic Pd-Pt catalysts (0.5 wt% total metal load) supported on sulfated zirconia were synthesized and tested in the gas-phase hydrodechlorination of chloromethanes. STEM images confirm the presence of well dispersed bimetallic particles. Besides their high activity, the main feature of these catalysts was their stability demonstrated in long term experiments. TOF values in the range of 0.0007 to 0.0168 s^{-1} and apparent activation energies between 41.1 kJ·mol^{-1} for SZ Pt-Pd (1:3) to 43.9 kJ·mol^{-1} for SZ Pt-Pd (3:1) were obtained for the dechlorination of DCM. The TOF values increased at increasing mean metal particle size within the range studied in this work (≈1.2-2.3 nm). The catalyst

with the higher proportion of Pt showed lower global activity and TOF. All the catalysts tested yielded similar patterns in terms of selectivity, being methane by far the main reaction product, although significant relative amounts of ethane and propane were also obtained. A very slight variation of the metal particle size was observed after reaction, supporting the high stability of these bimetallic catalysts. The good performance of the catalysts was demonstrated also with complex mixtures of several chloromethanes.
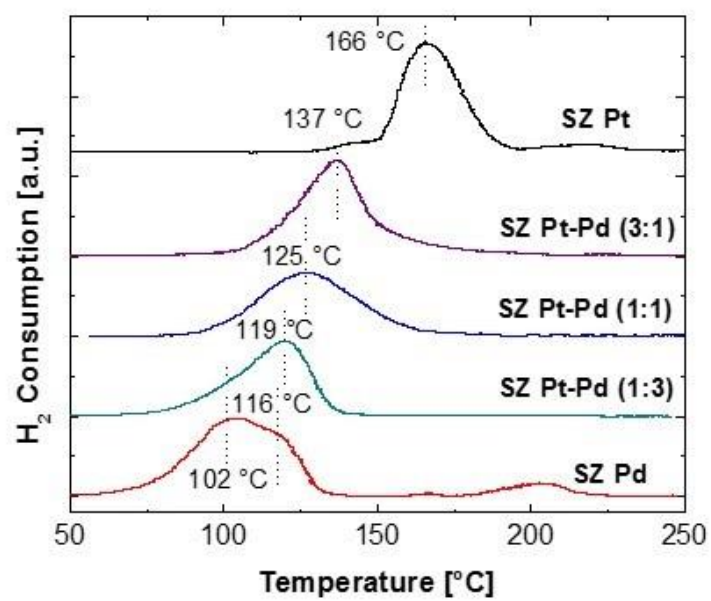
Figure 1. TPR profiles of the catalysts.
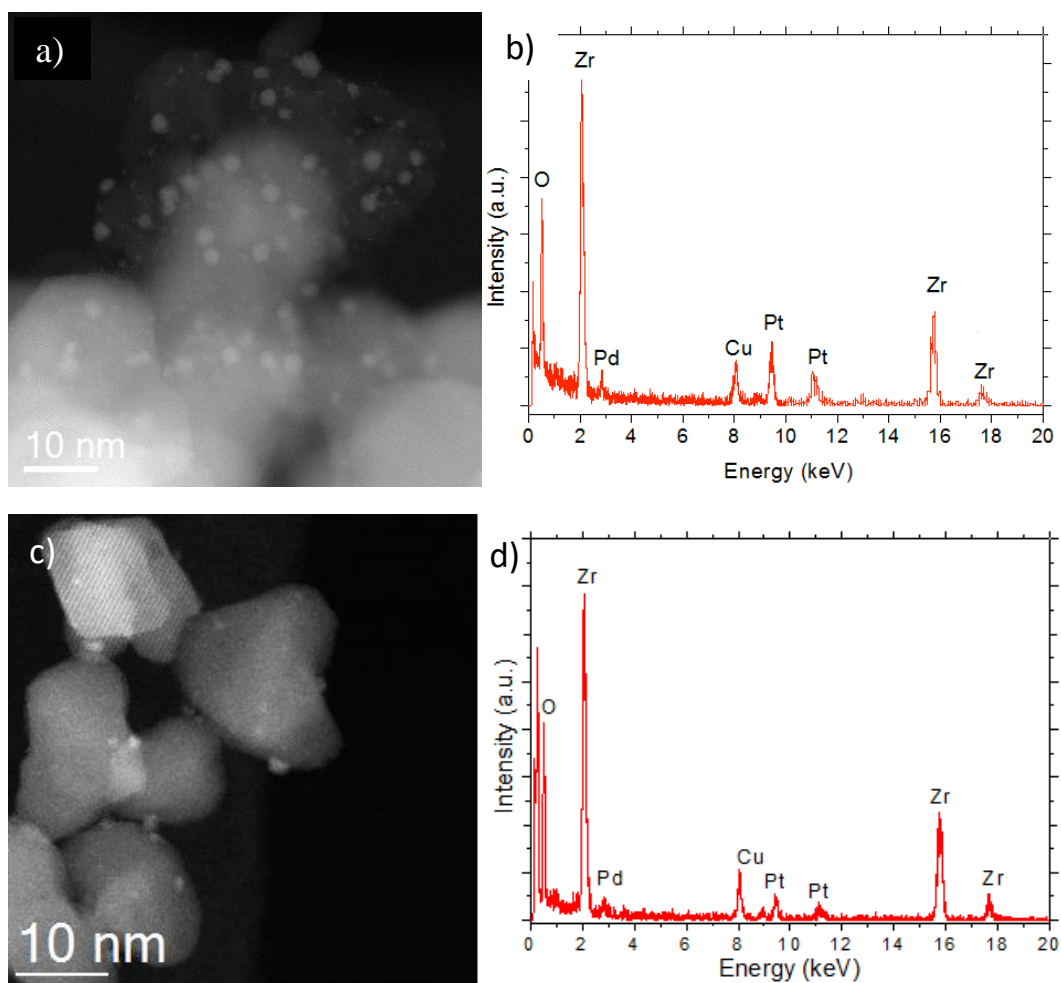
Figure 2. Representative C$_s$-corrected STEM-HAADF images of SZ Pt-Pd (1:1) and SZ Pt-Pd (1:3) catalysts (a and c) and their corresponding EDS analyses (b and d).
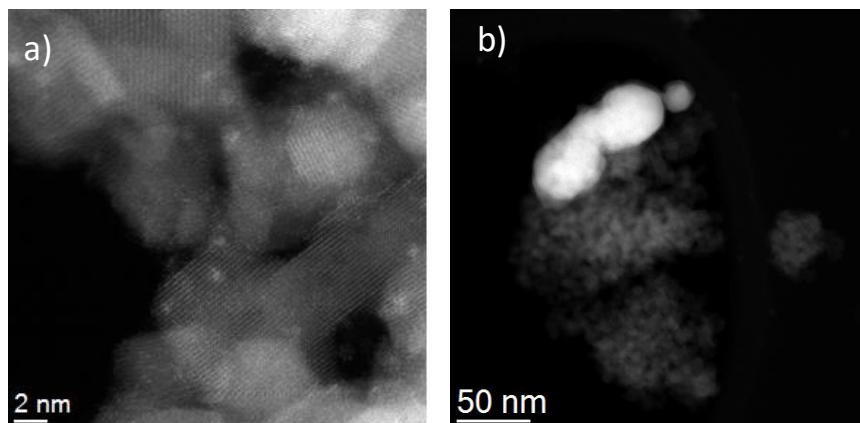
Figure 3. Representative C$_s$-corrected STEM-HAADF images of well dispersed (a) and higher size (b) metallic nanoparticles of SZ Pt-Pd (3:1).
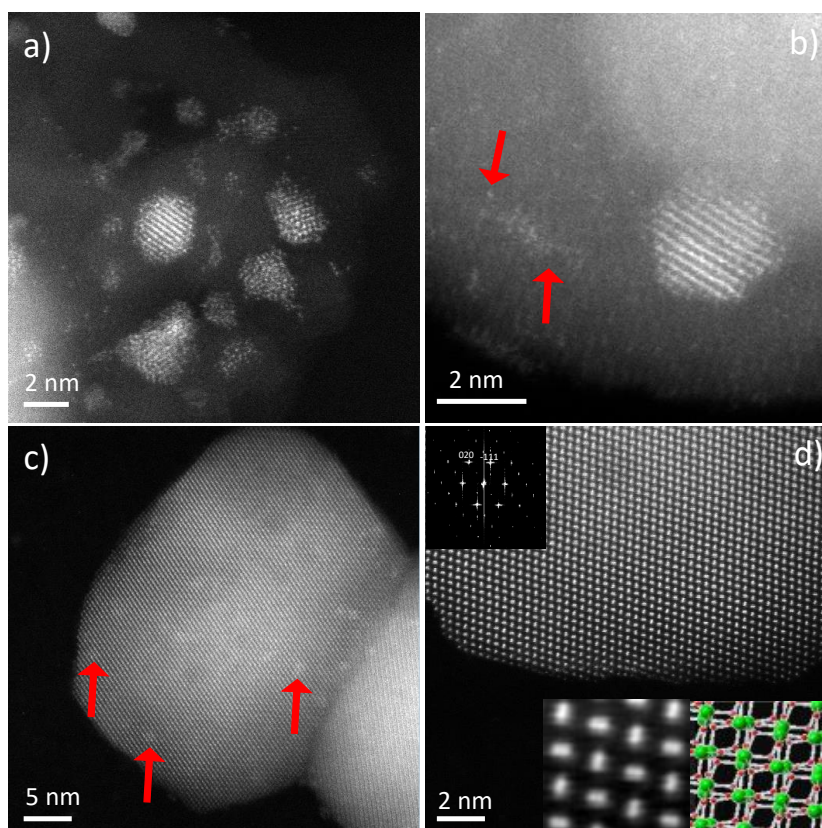
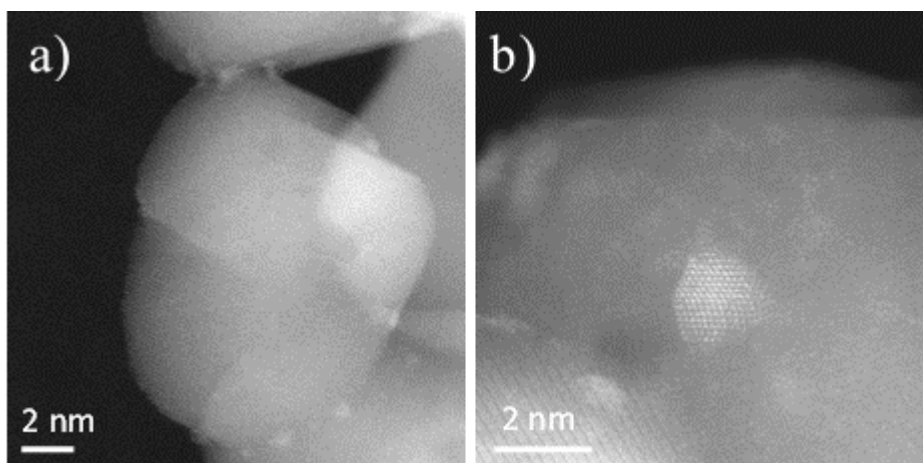**Figure 4.** High magnification C_s-corrected STEM-HAADF images of SZ Pt:Pd (1:1) (red arrows denoting isolated metal atoms).

Figure 5. C_s-corrected STEM-HAADF images: a) Low-magnification image of a ZrO_2 crystal with several metal nanoparticles on the surface. b) Atomic-resolution data of an *fcc* 2 nm nanoparticle, where isolated atoms can be also identified.[2]
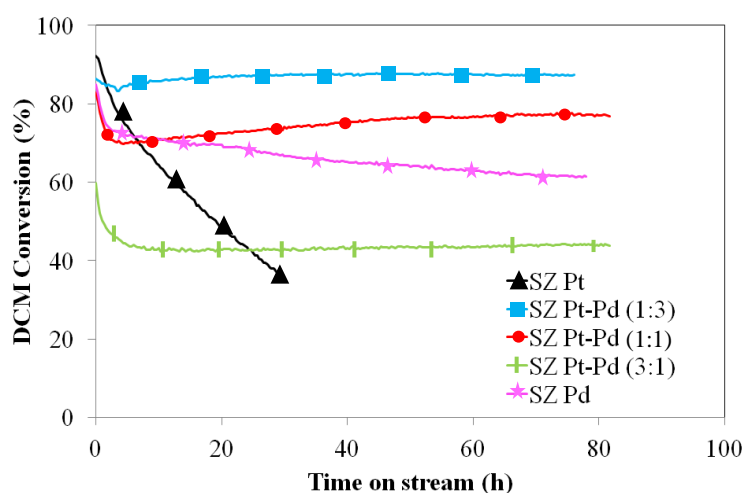

Figure 6. Evolution of DCM conversion upon time on stream in long-term experiments with the catalysts tested (space time = 0.8 $kg_{cat} \cdot h \cdot mol^{-1}$; T = 250 ºC).
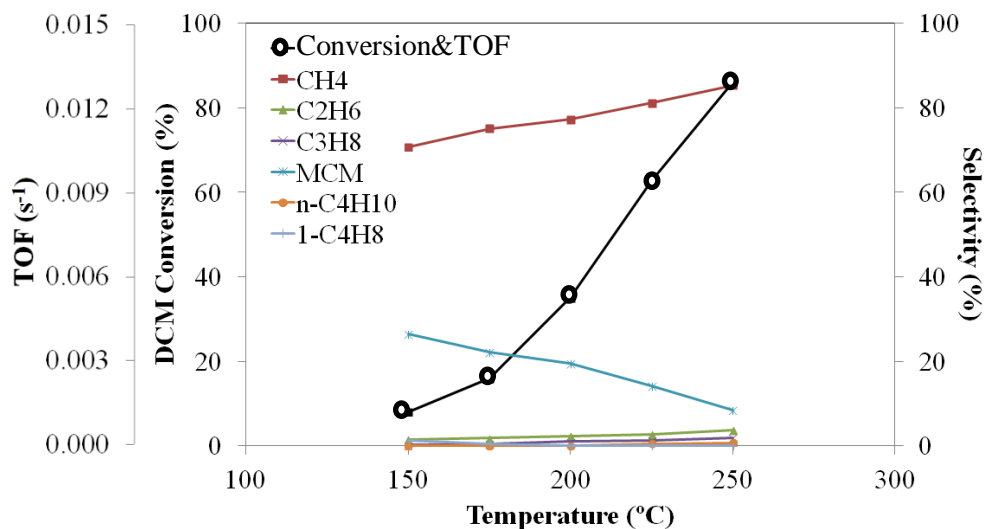
Figure 7. Results from DCM HDC with SZ Pt-Pd (1:3) at different temperatures (1000 ppmv inlet concentration and 0.8 $kg_{cat} \cdot h \cdot mol^{-1}$ space time).
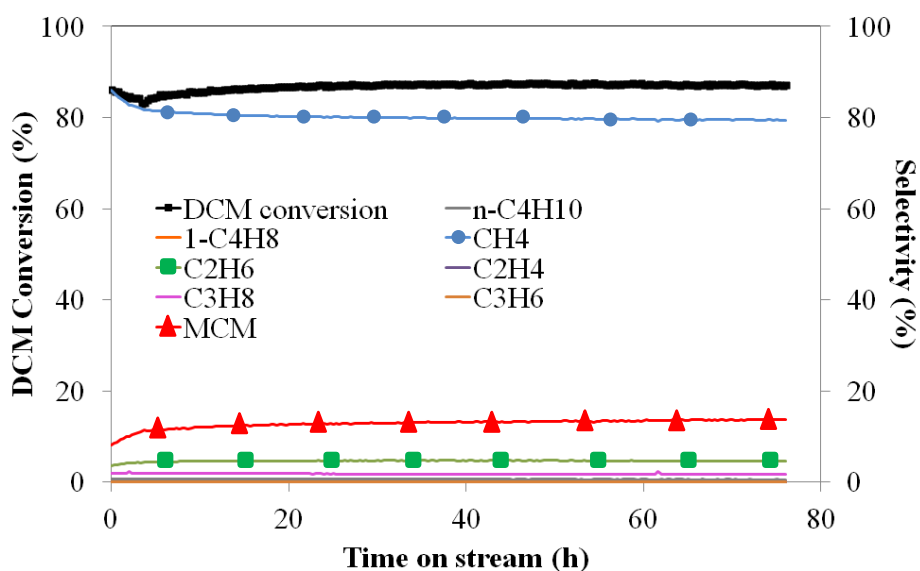

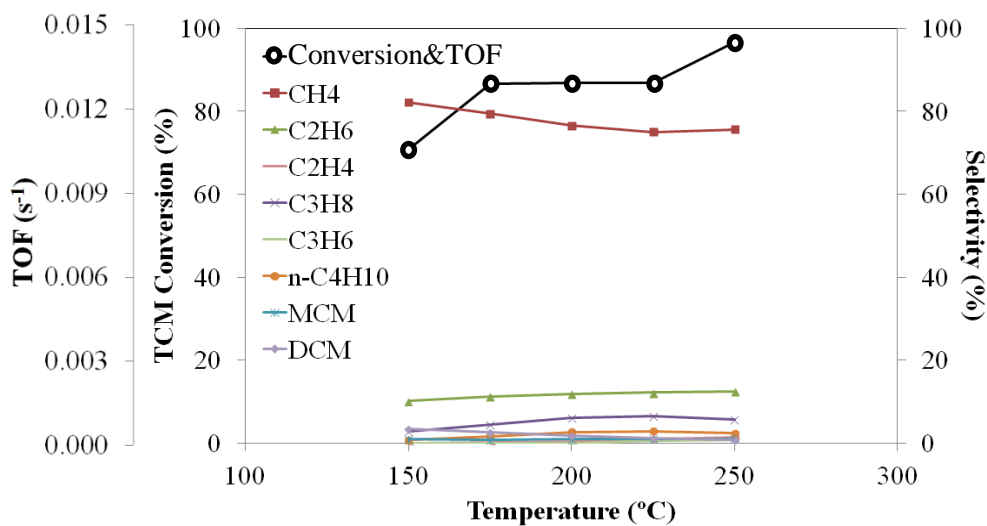**Figure 8.** Results of DCM HDC with SZ Pt-Pd (1:3) upon time on stream at 250 °C and 0.8 $kg_{cat} \cdot h \cdot mol^{-1}$ space time.

Figure 9. Results from TCM HDC with SZ Pt-Pd (1:3) at different temperatures (1000 ppmv inlet concentration and 0.8 kg$_{cat}$·h·mol^{-1} space time).
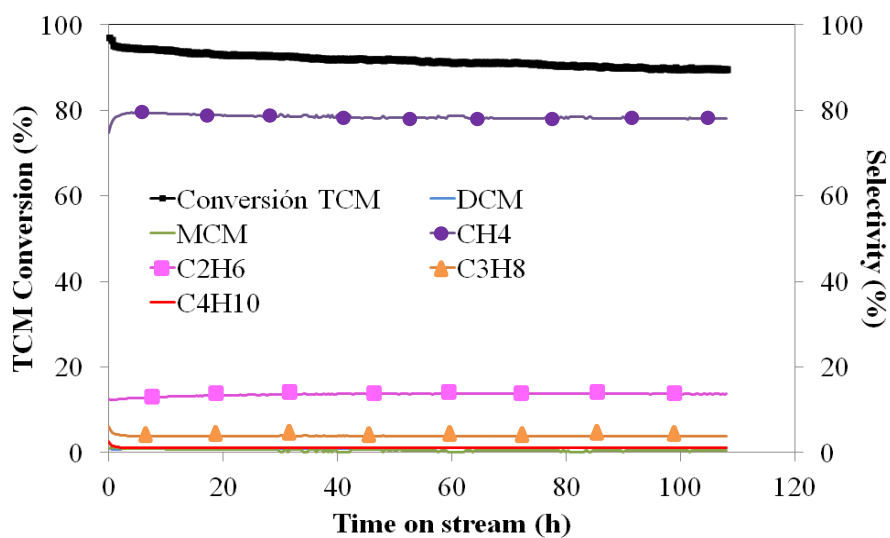
Figure 10. Results of TCM HDC with SZ Pt-Pd (1:3) upon time on stream at 250 ºC

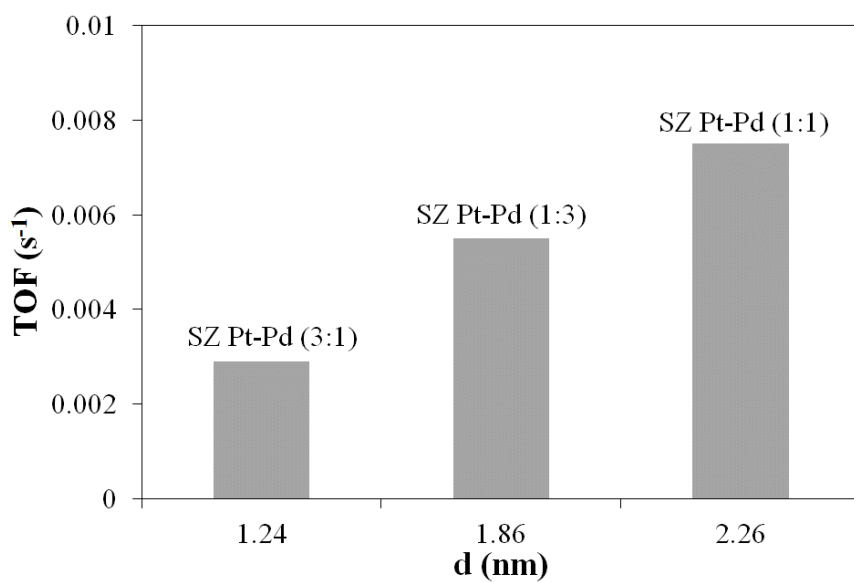and 0.8 $kg_{cat} \cdot h \cdot mol^{-1}$ space time.

Figure 11. TOF values for the HDC of DCM at 200 ºC versus the mean particle size
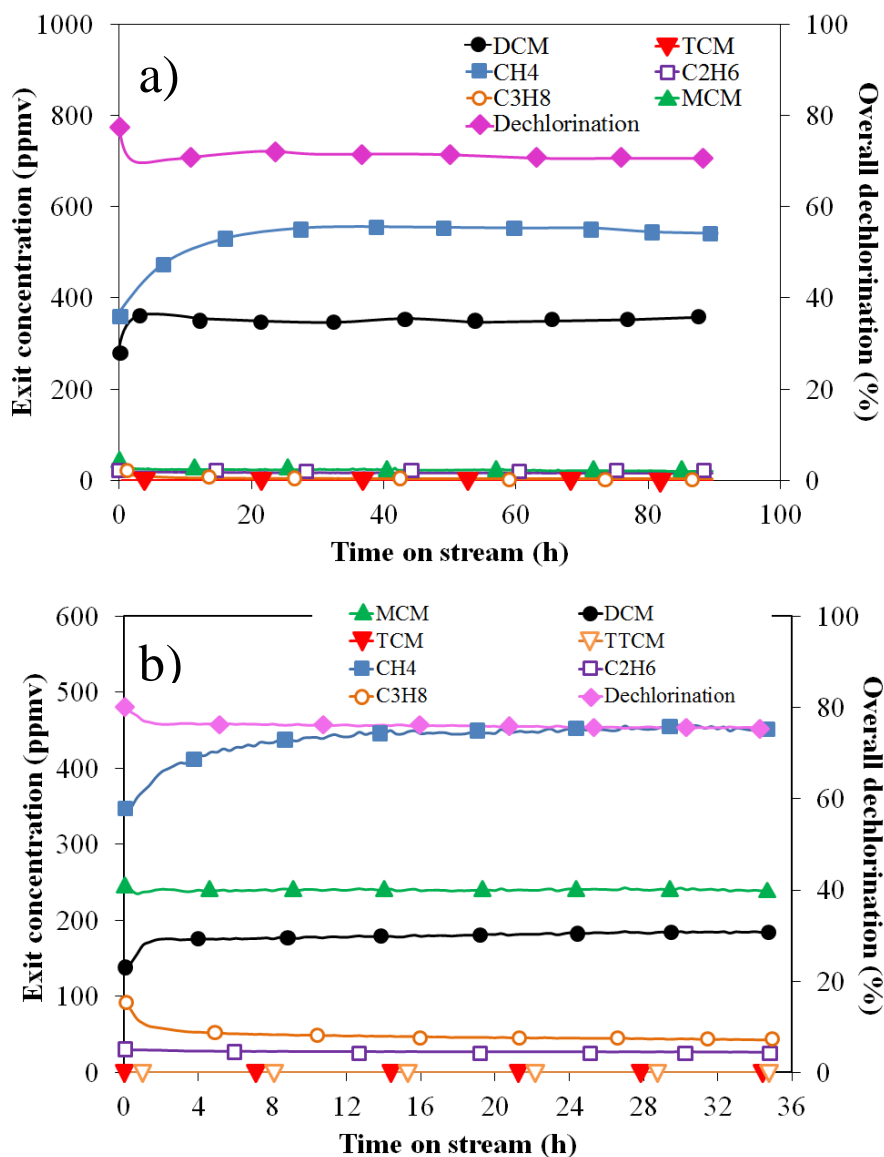
obtained by TEM for the three bimetallic catalysts.

Figure 12. Evolution of exit concentrations and overall dechlorination upon time on stream in the HDC of mixtures of (a) TCM and DCM (both at 500 ppmv inlet concentration), and (b) TTCM, TCM, DCM and MCM (all at 250 ppmv inlet concentrations) with the SZ Pt-Pd (1:3) catalyst at 250 ºC and 0.8 $kg_{cat} \cdot h \cdot mol^{-1}$ space time.

References

[1] E. Dobrzynska, M. Posniak, M. Szewczynska, B. Buszewski, Chlorinated Volatile Organic compounds-Old, however, actual analytical and toxicological problem, Crit. Rev. Anal. Chem. 40 (2010) 41-57.

[2] E. Lopez, S. Ordoñez, F.V. Diez, Deactivation of a Pd/Al$_2$O$_3$ catalyst used in hydrodechlorination reactions: Influence of the nature of organochlorinated compound and hydrogen chloride, Appl. Catal. B Environ. 62 (2006) 57-65.

[3] T. Mori, T. Kikuchi, J. Kubo, Y. Morikawa, Hydrodechlorination of trichloromethane to higher hydrocarbons over Pd/SiO$_2$ catalyst, Chem. Lett. 30 (2001) 936-938.

[4] B. Aristizabal, C.A. Gonzalez, I. Barrio, M. Montes, C.M. de Correa, Screening of Pd and Ni supported on sol-gel derived oxides for dichloromethane hydrodechlorination, J. Mol. Catal. A Chem. 222 (2004) 189-198.

[5] C.A. Gonzalez, M. Bartoszek, A. Martin, C. Montes de Correa, Hydrodechlorination of light organochlorinated compounds and their mixtures over Pd/TiO$_2$-washcoated minimonoliths, Ind. Eng. Chem. Res. 48 (2009) 2826-2835.

[6] C.A. Gonzalez, C.O.M. Patino, C. Montes de Correa. Catalytic hydrodechlorination of dichloromethane in the presence of traces of chloroform and tetrachloroethylene, Catal. Today 133–135 (2008) 520-525.

[7] B. Heinrichs, F. Noville, J. Schoebrechts, J. Pirard, Palladium-silver sol-gel catalysts for selective hydrodechlorination of 1,2-dichloroethane into ethylene: IV. Deactivation mechanism and regeneration, J. Catal. 220 (2003) 215-225.

[8] D. Chakraborty, P.P. Kulkarni, V.I. Kovalchuk, J.L. d'Itri, Dehalogenative oligomerization of dichlorodifluoromethane catalyzed by activated carbon-supported Pt-Cu catalysts: effect of Cu to Pt atomic ratio, Catal. Today 88 (2004) 169-181.

[9] M. Legawiec-Jarzyna, A. Srebowata, W. Juszczyk, Z. Karpinski, Hydrodechlorination of dichlorofluoromethane, carbon tetrachloride and 1,2-dichloroethane over Pt/Al$_2$O$_3$ catalysts, J. Mol. Catal. A Chem. 224 (2004) 171-177.

[10] C. Amorim, G. Yuan, P.M. Patterson, M.A. Keane, Catalytic hydrodechlorination over Pd supported on amorphous and structured carbon, J. Catal. 234 (2005) 268-281.

[11] S. Ordóñez, E. Díaz, R.F. Bueres, E. Asedegbega-Nieto, H. Sastre, Carbon nanofibre-supported palladium catalysts as model hydrodechlorination catalysts, J. Catal. 272 (2010) 158-168.

[12] B. Coq, S. Hub, F. Figueras, D. Tournigant, Conversion under hydrogen of dichlorodifluoromethane over bimetallic palladium catalysts, Appl. Catal. A: Gen. 101 (1993) 41–50.

[13] M. Bonarowska, Z. Kaszkur, D. Łomot, M. Rawski, Z. Karpinska, Effect of gold on catalytic behavior of palladium catalysts in hydrodechlorination of tetrachloromethane, Appl. Catal. B: Environ. 162 (2015) 45–56.

[14] N. Seshu Babu, N. Lingaiah, P.S. Sai Prasad, Characterization and reactivity of Al_2O_3 supported Pd-Ni bimetallic catalysts for hydrodechlorination of chlorobenzene, Appl. Catal. B: Environ. 111–112 (2012) 309–316.

[15] Y. Han, G. Gu, J. Sun, W. Wang, H. Wan, Z. Xu, S. Zheng, Selective hydrodechlorination of 1,2-dichloroethane to ethylene over Pd-Ag/Al2O3 catalysts prepared by surface reduction, Appl. Surf. Sci. 355 (2015) 183–190.

[16] B.T. Meshesha, N. Barrabés, J. Llorca, A. Dafinov, F. Medina, K. Föttinger, PdCu alloy nanoparticles on alumina as selective catalysts for trichloroethylene hydrodechlorination to ethylene, Appl. Catal. A: Gen. 453 (2013) 130–141.

[17] G. Yuan, C. Louis, L. Delannoy, M.A. Keane, Silica- and titania-supported Ni-Au: Application in catalytic hydrodechlorination, J. Catal. 247 (2007) 256-268.

[18] M. Legawiec-Jarzyna, W. Juszczyk, M. Bonarowska, Z. Kaszkur, L. Kepinski, Z. Kowalczyk, Z. Karpinski, Hydrodechlorination of CCl_4 on Pt-Au/Al_2O_3 catalysts, Top. Catal. 52 (2009) 1037-1043.

[19] M Martin-Martinez, L.M. Gómez-Sainero, J. Bedia, A. Arevalo-Bastante, J.J. Rodriguez, Enhanced activity of carbon-supported Pd-Pt catalysts in the hydrodechlorination of dichloromethane, Appl. Catal. B: Environ. 184 (2016) 55-63.

[20] J. Bedia, L.M. Gómez-Sainero, J.M. Grau, M. Busto, M. Martin-Martinez, J.J. Rodríguez, Hydrodechlorination of dichlormethane with mono- and bimetallic Pd-Pt on sulfated and tungstated zirconia catalysts, J. Catal. 294 (2012) 207-215.

[21] S. Brunauer, P.H. Emmett, E. Teller, Surface area measurements of activated carbon, silica gels and other adsorbents, J. Am. Chem. Soc. 60 (1938) 309-319.

[22] C.H. Bartholomew, R.B. Pannell, The stoichiometry of hydrogen and carbon monoxide chemisorption on alumina- and silica-supported nickel, J. Catal. 65 (1980) 390-401.

[23] R. Navarro, B. Pawelec, J.M. Trejo, R. Mariscal, J.L.G. Fierro, Hydrogenation of aromatics on sulfur-resistant PtPd bimetallic catalysts, J. Catal. 189 (2000) 184-194.

[24] V.L. Barrio, P.L. Arias, J.F. Cambra, M.B. Güemez, B. Pawelec, J.L.G. Fierro, Aromaticshydrogenation on silica-alumina supported palladium-nickel catalysts, Appl. Catal. A 242 (2003) 17-30.

[25] J.F. Moulder, W.F. Stickle, P.E. Sobol, K.D. Bomben, in: J. Chastain, R.C. King Jr. (Eds.), Handbook of X-ray Photoelectron Spectroscopy, Physical Electronics, Inc., Eden Prairie, MN, 1995.

[26] A.M. Garrido Pedrosa, M.J.B. Souza, B.A. Marinkovic, D.M.A. Melo, A.S. Araujo, Structure and properties of bifunctional catalysts based on zirconia modified by tungsten oxide obtained by polymeric precursor method, Appl. Catal A Gen. 342 (2008) 56-62.

[27] K. Persson, A. Ersson, S. Colussi, A. Trovarelli, S.G. Järås, Catalytic combustion of methane over bimetallic Pd-Pt catalysts: The influence of support materials, Appl. Catal B Environ 66 (2006) 175-185.

[28] L. Calvo, A.F. Mohedano, J.A. Casas, M.A. Gilarranz, J.J. Rodríguez, Treatment of chlorophenols-bearing wastewaters through hydrodechlorination using Pd/activated carbon catalysts, Carbon 42 (2004) 1371-1375.

[29] L. Calvo, M.A. Gilarranz, J.A. Casas, A.F. Mohedano, J.J. Rodríguez, Effects of support surface composition on the activity and selectivity of Pd/C catalysts in aqueous-phase hydrodechlorination reactions, Ind. Eng. Chem. Res. 44 (2005) 6661-6667.

[30] J. Bedia, J.M. Rosas, J. Rodríguez-Mirasol, T. Cordero, Pd supported on mesoporous activated carbons with high oxidation resistance as catalysts for toluene oxidation, Appl. Catal. B: Environ. 94 (2010) 8-18.

[31] A. Mayoral, L. F. Allard, D. Ferrer, R. Esparza, M. Jose-Yacaman, On the behavior of Ag nanowires under high temperature: in situ characterization by aberration-corrected STEM, J. Mater. Chem. 21 (2011) 893-898

[32] A. Mayoral, T. Carey, P. A. Anderson, I. Diaz, Atomic resolution analysis of porous solids: A detailed study of silver ion-exchanged zeolite A, Micropor. Mesopor. Mater. 116 (2013) 117–122.

[33] T. Mori, T. Yasuoka, Y. Morikawa, Hydrodechlorination of 1,1,2-trichloro-1,2,2-trifluoroeethane (CFC-113) over supported ruthenium and other noble metal catalysts, Catal. Today 88 (2004) 111-120.

[34] M. Martin-Martinez, L.M. Gómez-Sainero, M.A. Alvarez-Montero, J. Bedia, J.J. Rodriguez, Comparison of different precious metals in activated carbon-supported catalysts for the gas-phase hydrodechlorination of chloromethanes, Appl. Catal. B: Environ. 132– 133 (2013) 256–265.

[35] T. Mori, K. Hirose, T. Kikuchi, J. Kubo, Y. Morikawa, Formation of higher hydrocarbons from chloromethanes via hydrodechlorination over Pd/SiO$_2$ catalyst, J. Jpn. Pet. Inst. 45 (2002) 256–259.

[36] M.A. Alvarez-Montero, L.M. Gomez-Sainero, M. Martin-Martinez, F. Heras, J.J: Rodriguez, Hydrodechlorination of chloromethanes with Pd on activated carbon catalysts for the treatment of residual gas streams, Appl Catal. B. Environ. 96 (2010) 148-156.

[37] M. Bonarowska, A. Malinowski, Z. Karpínski. Hydrogenolysis of C–C and C–Cl bonds by Pd–Re/Al$_2$O$_3$ catalysts. Applied Catalysis A: General 188 (1999) 145–154

[38] M.A. Álvarez-Montero, L.M. Gómez-Sainero, A. Mayoral, I. Diaz, R.T. Baker, J.J. Rodriguez. Hydrodechlorination of chloromethanes with a highly stable Pt on activated carbon catalyst. Journal of Catalysis 279 (2011) 389–396

[39] E. López, S. Ordonez, H. Sastre, F.V. Diez, Kinetic study of the gas-phase hydrogenation of aromatic and aliphatic organochlorinated compounds using a Pd/Al$_2$O$_3$ catalyst, J. Hazard. Mater. 97 (1–3) (2003) 281–294.

[40] A. Arevalo-Bastante, M.A. Álvarez-Montero, J. Bedia, L.M. Gómez-Sainero, J.J. Rodriguez, Gas-phase hydrodechlorination of mixtures of chloromethanes with activated carbon-supported platinum catalysts, Appl. Catal. B: Environ. 179 (2015) 551–557

[41] S. Ordonez, F.V. Diez, H. Sastre, Catalytic hydrodechlorination of chlorinated olefins over a Pd/Al$_2$O$_3$ catalyst: kinetics and inhibition phenomena, Ind. Eng. Chem. 41 (2002) 505–511.